Substructure decoupling without using rotational DoFs: fact or fiction?

Walter D'Ambrogio[a], Annalisa Fregolent[b,*]

[a]*Dipartimento di Ingegneria Industriale e dell'Informazione e di Economia, Università dell'Aquila, Via G. Gronchi, 18 - I-67100, L'Aquila (AQ), Italy*
[b]*Dipartimento di Ingegneria Meccanica e Aerospaziale, Università di Roma La Sapienza, Via Eudossiana, 18 - I-00184 Roma, Italy*

Abstract

In the framework of experimental dynamic substructuring, substructure decoupling consists in the identification of the dynamic behaviour of a structural subsystem, starting from the dynamic behaviour of both the assembled system and the residual subsystem (the known portion of the assembled system). On the contrary, substructure coupling identifies an assembled system starting from the component subsystems. The degrees of freedom (DoFs) of the assembled system can be partitioned into internal DoFs (not belonging to the couplings) and coupling DoFs.

In substructure coupling, whenever coupling DoFs include rotational DoFs, the related rotational FRFs must be obtained experimentally. Does this requirement holds for substructure decoupling too, as it is commonly believed?

Decoupling can be ideally accomplished by adding the negative of the residual subsystem to the assembled system (direct decoupling) and by enforcing compatibility and equilibrium at enough interface DoFs. Ideally, every DoF of the residual subsystem belongs to the interface between the assembled system and the residual subsystem. Hopefully, not all the coupling DoFs are necessary to enforce compatibility and equilibrium. This may allow to skip coupling DoFs and specifically rotational DoFs.

The goal of the paper is indeed to establish if rotational FRFs at coupling DoFs can be neglected in substructure decoupling. To this aim, after highlighting the possibility of avoiding the use of coupling DoFs from a theoretical standpoint, a test bed coupled through flexural and torsional DoFs is considered. Experimental results are presented and discussed.

Keywords: Substructure Decoupling, Rotational DoFs, Mixed Interface, Experimental Dynamic Substructuring

1. Introduction

The objective of this paper is to establish whether rotational FRFs at coupling DoFs can be neglected in substructure decoupling, or on the contrary they are an essential requirement as in substructure coupling. An original contribution of this paper is to provide an answer to this question from a theoretical standpoint and to verify it on an experimental test case.

Substructure decoupling consists in the identification of the dynamic behaviour of a structural subsystem, starting from the dynamic behaviour of both the assembled system and the residual subsystem (the known portion of the assembled system). Decoupling is a need for subsystems that cannot be measured separately, but only when coupled to their neighboring substructure(s) (e.g. fixtures needed for testing or subsystems in operational conditions). On the contrary, substructure coupling identifies an assembled system starting from the component subsystems.

Substructure decoupling represents a special case of experimental dynamic substructuring, where 'experimental' implies that the model of at least one subsystem derives from tests. In Frequency Based Substructuring, Frequency Response Functions (FRFs) are used instead of modal parameters to avoid modal truncation problems. A general framework for dynamic substructuring is provided in [1], where the concept of primal and dual assembly is introduced.

*Corresponding author
Email addresses: walter.dambrogio@univaq.it (Walter D'Ambrogio), annalisa.fregolent@uniroma1.it (Annalisa Fregolent)

Preprint, published in Mechanical Systems and Signal Processing ***72-73****(2016), 499-512*

A well known issue in experimental dynamic substructuring is related to rotational DoFs. In substructure coupling, whenever coupling DoFs include rotational DoFs, the related rotational FRFs must be obtained experimentally. This becomes a quite complicated task when measuring only translational FRFs, as shown in [2]. Several techniques for measuring rotational responses have been devised, see e.g. [3, 4]. However, are rotational DoFs essential for substructure decoupling, as one could believe? An answer will be provided after having considered if and how substructure decoupling techniques differ from substructure coupling techniques.

Substructure decoupling techniques can be classified as reverse coupling techniques or direct decoupling techniques. In reverse coupling, the equations written for the coupling problem are rearranged to isolate (as unknown) one of the substructures instead of the assembled structure. Examples of reverse coupling are impedance and mobility approaches [5, 6].

In direct decoupling, a negative structure, i.e. a fictitious subsystem that is the negative of the residual subsystem, is added to the assembled system. Appropriate compatibility and equilibrium conditions are enforced at interface DoFs. To solve the decoupling problem, dual assembly [7], primal assembly [8] or hybrid assembly [9] can be used. Compatibility and equilibrium can be required either at coupling DoFs only (standard interface), or at additional internal DoFs of the residual subsystem (extended interface), or at subsets of coupling DoFs and internal DoFs of the residual subsystem (mixed interface), or at a subset of internal DoFs of the residual subsystem only (pseudo interface).

In the framework of direct decoupling, the known FRFs of the assembled system implicitly account for forces and moments transmitted through the coupling DoFs. The effect of the negative structure is to add a set of disconnection forces [10] at interface DoFs: note that interface DoFs are not necessarily the same as coupling DoFs. However, disconnection forces are such as to cancel forces and moments exchanged through the coupling DoFs. Therefore, a mixed interface [11] or a pseudo interface can be considered that allow to substitute undesired coupling DoFs with internal DoFs of the residual subsystem that are amenable to measurement. This approach was preliminarily introduced in [12] using simulated test data and in [13] using experimental data.

The paper is organized as follows. In section 2, the direct decoupling problem is presented and the possibility of avoiding the use of coupling DoFs is highlighted. In section 3, a tree structure is considered made by a cantilever column with two staggered short arms coupled to a horizontal beam: measurements performed to obtain the experimental FRFs on the assembled structure and on the residual substructure (cantilever column) are described too. In section 4, the FRFs of the unknown substructure (horizontal beam) are identified using the described decoupling procedure, in which rotational DoFs are neglected and substituted by internal translational DoFs: raw experimental FRFs and curve fitted FRFs are alternatively considered.

2. Direct decoupling using dual assembly

The unknown substructure U (N_U DoFs) is a portion of a larger structure RU (N_{RU} DoFs). The known portion of the assembled structure RU, defined as residual substructure R (N_R DoFs), is joined to the unknown substructure through a number of couplings (see Fig. 1). The degrees of freedom (DoFs) can be partitioned into internal DoFs (not belonging to the couplings) of substructure U (u), internal DoFs of substructure R (r), and coupling DoFs (c).

The goal is to find the FRF of the unknown substructure U starting from the FRFs of the assembled structure RU and of the residual substructure R. The dynamic behaviour of the unknown substructure U can be extracted from that of the assembled structure RU by taking out the dynamic effect of the residual subsystem R. This can be accomplished by considering a negative structure, i.e. by adding to the assembled structure RU a fictitious substructure with a dynamic stiffness opposite to that of the residual substructure R and satisfying compatibility and equilibrium conditions. The dynamic equilibrium of the assembled structure RU and of the negative substructure is expressed in block diagonal format as:

$$\begin{bmatrix} \mathbf{Z^{RU}} & \mathbf{0} \\ \mathbf{0} & -\mathbf{Z^{R}} \end{bmatrix} \begin{Bmatrix} \boldsymbol{u}^{RU} \\ \boldsymbol{u}^{R} \end{Bmatrix} = \begin{Bmatrix} \boldsymbol{f}^{RU} \\ \boldsymbol{f}^{R} \end{Bmatrix} + \begin{Bmatrix} \boldsymbol{g}^{RU} \\ \boldsymbol{g}^{R} \end{Bmatrix} \tag{1}$$

where:

- $\mathbf{Z^{RU}}$, $-\mathbf{Z^{R}}$ are the dynamic stiffness matrices of the assembled structure RU and of the negative structure, respectively;

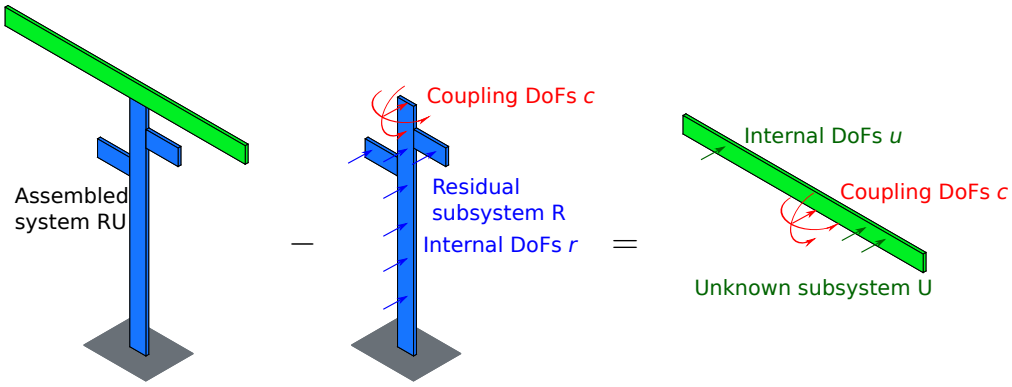

Figure 1: Scheme of the direct decoupling problem.

- $\boldsymbol{u}^{RU}$, $\boldsymbol{u}^{R}$ are the vectors of degrees of freedom of the assembled structure RU and of the negative structure, respectively;
- $\boldsymbol{f}^{RU}$, $\boldsymbol{f}^{R}$ are the external force vectors on the assembled structure RU and on the negative structure, respectively;
- $\boldsymbol{g}^{RU}$, $\boldsymbol{g}^{R}$ are the vectors of disconnection forces exchanged between the assembled structure and the negative structure (constraint forces associated with compatibility conditions).

Compatibility and equilibrium conditions must be considered at the interface between the assembled structure RU and the negative structure: such interface includes not only the coupling DoFs between substructures U and R, but includes as well the internal DoFs of substructure R (the blue part of the structure in Fig. 1). However, it is not required to consider the full set of these interface DoFs, because it is sufficient that the number of interface DoFs be not less than the number of coupling DoFs n_c. Therefore, several options for interface DoFs can be considered:

- standard interface, including only the coupling DoFs (c) between substructures U and R;
- extended interface, including also a subset of internal DoFs ($i \subseteq r$) of the residual substructure R;
- mixed interface, including subsets of coupling DoFs ($d \subset c$) and internal DoFs ($i \subseteq r$) of substructure R;
- pseudo interface, including only internal DoFs ($i \subseteq r$) of substructure R.

The use of a mixed or pseudo interface may allow to ignore rotational coupling DoFs by substituting them with translational internal DoFs.

The compatibility condition at the (standard, extended, mixed, pseudo) interface DoFs implies that any pair of matching DoFs u_l^{RU} and u_m^R, i.e. DoF l on the coupled system RU and DoF m on subsystem R must have the same displacement, that is $u_l^{RU} - u_m^R = 0$. Let the number of interface DoFs on which compatibility is enforced be denoted as N_C.

The compatibility condition can be generally expressed as:

$$\begin{bmatrix} \mathbf{B}_\mathbf{C}^{\mathbf{RU}} & \mathbf{B}_\mathbf{C}^{\mathbf{R}} \end{bmatrix} \begin{Bmatrix} \boldsymbol{u}^{RU} \\ \boldsymbol{u}^{R} \end{Bmatrix} = \mathbf{0} \tag{2}$$

where each row of $\mathbf{B_C} = \begin{bmatrix} \mathbf{B}_\mathbf{C}^{\mathbf{RU}} \mathbf{B}_\mathbf{C}^{\mathbf{R}} \end{bmatrix}$ corresponds to a pair of matching DoFs. Note that $\mathbf{B_C}$ has size $N_C \times (N_{RU} + N_R)$ and is, in most cases, a signed Boolean matrix.

It should be noted that the interface DoFs involved in the equilibrium condition need not to be the same used to enforce the compatibility condition, as long as compatibility can be ensured by disconnection forces applied at a

different set of DoFs. If the compatibility and the equilibrium DoFs are not the same, the approach is called non-collocated [11]. Obviously, the traditional approach, in which compatibility and equilibrium DoFs are the same, is called collocated.

Let N_E denote the number of interface DoFs on which equilibrium is enforced. The equilibrium of disconnection forces implies that their sum must be zero for any pair of matching DoFs belonging to the equilibrium interface, i.e. $g_r^{RU} + g_s^R = 0$. Furthermore, for any DoF k on the coupled system RU (or on the residual subsystem R) not belonging to the equilibrium interface, it must be $g_k^{RU} = 0$ ($g_k^R = 0$).

Overall, the above conditions can be expressed as:

$$\begin{bmatrix} \mathbf{L_E^{RU}} \\ \mathbf{L_E^R} \end{bmatrix}^T \begin{Bmatrix} \boldsymbol{g}^{RU} \\ \boldsymbol{g}^R \end{Bmatrix} = \mathbf{0} \tag{3}$$

where the matrix $\mathbf{L_E} = \left[\mathbf{L_E^{RU}}\, \mathbf{L_E^R}\right]$ is a Boolean localisation matrix. Note that the number of columns of $\mathbf{L_E}$ is equal to the number N_E of equilibrium interface DoFs plus the number N_{NE} of DoFs not belonging to the equilibrium interface. Note that $N_{NE} = N_{RU} + N_R - 2N_E$: in fact, the number of DoFs belonging to the equilibrium interface must be subtracted once from N_{RU} and once from N_R. Therefore, the size of $\mathbf{L_E}$ is $(N_{RU} + N_R) \times (N_{RU} + N_R - N_E)$.

Eqs. (1-3) can be gathered to obtain the so-called 3-field formulation. Starting from the 3-field formulation, several assembly techniques can be devised:

- dual assembly [1, 7] where equilibrium is satisfied exactly by defining a unique set of disconnection force intensities;
- primal assembly [1, 8] where compatibility is satisfied exactly by defining a unique set of interface DoFs;
- hybrid assembly [9] where both compatibility and equilibrium are satisfied exactly.

In the sequel, only the dual assembly is recalled. It can be shown [9] that whenever $N_C = N_E$, i.e. the number of compatibility DoFs is the same as the number of equilibrium DoFs, all assembly techniques provide the same result.

2.1. Dual assembly

In the dual assembly, the equilibrium condition $g_r^{RU} + g_s^R = 0$ at a pair of equilibrium interface DoFs is ensured by choosing $g_r^{RU} = -\lambda$ and $g_s^R = \lambda$. If a Boolean matrix $\mathbf{B_E}$ related to interface equilibrium DoFs is defined similarly to $\mathbf{B_C}$, the overall interface equilibrium can be ensured by writing the disconnection forces in the form:

$$\begin{Bmatrix} \boldsymbol{g}^{RU} \\ \boldsymbol{g}^R \end{Bmatrix} = -\begin{bmatrix} \mathbf{B_E^{RU}}^T \\ \mathbf{B_E^R}^T \end{bmatrix} \boldsymbol{\lambda} \tag{4}$$

where $\boldsymbol{\lambda}$ are Lagrange multipliers corresponding to disconnection force intensities and $\mathbf{B_E}$ is a $N_E \times (N_{RU} + N_R)$ matrix. Since there is a unique set of disconnection force intensities $\boldsymbol{\lambda}$, the interface equilibrium condition is satisfied automatically for any $\boldsymbol{\lambda}$, i.e.

$$\begin{bmatrix} \mathbf{L_E^{RU}} \\ \mathbf{L_E^R} \end{bmatrix}^T \begin{Bmatrix} \boldsymbol{g}^{RU} \\ \boldsymbol{g}^R \end{Bmatrix} = -\begin{bmatrix} \mathbf{L_E^{RU}} \\ \mathbf{L_E^R} \end{bmatrix}^T \begin{bmatrix} \mathbf{B_E^{RU}}^T \\ \mathbf{B_E^R}^T \end{bmatrix} \boldsymbol{\lambda} = \mathbf{0} \tag{5}$$

In the dual assembly, the total set of DoFs is retained, i.e. each interface DoF appears twice. Since Eq. (5) is always satisfied, the 3-field formulation reduces to:

$$\begin{cases} \begin{bmatrix} \mathbf{Z^{RU}} & \mathbf{0} \\ \mathbf{0} & -\mathbf{Z^R} \end{bmatrix} \begin{Bmatrix} \boldsymbol{u}^{RU} \\ \boldsymbol{u}^R \end{Bmatrix} + \begin{bmatrix} \mathbf{B_E^{RU}}^T \\ \mathbf{B_E^R}^T \end{bmatrix} \boldsymbol{\lambda} = \begin{Bmatrix} \boldsymbol{f}^{RU} \\ \boldsymbol{f}^R \end{Bmatrix} & (1^*) \\ \begin{bmatrix} \mathbf{B_C^{RU}} & \mathbf{B_C^R} \end{bmatrix} \begin{Bmatrix} \boldsymbol{u}^{RU} \\ \boldsymbol{u}^R \end{Bmatrix} = \mathbf{0} & (2) \end{cases}$$

or in more compact form:

$$\begin{cases} \mathbf{Z}\boldsymbol{u} + \mathbf{B_E}^T\boldsymbol{\lambda} = \boldsymbol{f} & (1^*) \\ \mathbf{B_C}\boldsymbol{u} = \mathbf{0} & (2) \end{cases}$$

To eliminate $\boldsymbol{\lambda}$, Eq. (1*) can be written:

$$\boldsymbol{u} = -\mathbf{Z}^{-1}\mathbf{B_E}^T\boldsymbol{\lambda} + \mathbf{Z}^{-1}\boldsymbol{f} \tag{6}$$

which substituted in Eq. (2) gives:

$$\mathbf{B_C}\mathbf{Z}^{-1}\mathbf{B_E}^T\boldsymbol{\lambda} = \mathbf{B_C}\mathbf{Z}^{-1}\boldsymbol{f} \tag{7}$$

from which $\boldsymbol{\lambda}$, to be back-substituted in Eq. (1*), is found as:

$$\boldsymbol{\lambda} = \left(\mathbf{B_C}\mathbf{Z}^{-1}\mathbf{B_E}^T\right)^+ \mathbf{B_C}\mathbf{Z}^{-1}\boldsymbol{f} \tag{8}$$

To obtain a determined or overdetermined matrix for the generalized inversion operation, the number of rows of $\mathbf{B_C}$ must be greater or equal than the number of rows of $\mathbf{B_E}$, i.e.

$$N_C \geq N_E \geq n_c \tag{9}$$

Note that, if $N_C > N_E$, Eq. (7) is not satisfied exactly by vector $\boldsymbol{\lambda}$ given by Eq. (8), but only in the minimum square sense. This implies that also Eq. (2) is not satisfied exactly, i.e. compatibility conditions at interface are approximately satisfied. On the contrary, equilibrium is satisfied exactly due to the introduction of the disconnection force intensities $\boldsymbol{\lambda}$ as in Eq. (4).

By substituting $\boldsymbol{\lambda}$ in Eq. (1*), it is obtained:

$$\mathbf{Z}\boldsymbol{u} + \mathbf{B_E}^T\left(\mathbf{B_C}\mathbf{Z}^{-1}\mathbf{B_E}^T\right)^+ \mathbf{B_C}\mathbf{Z}^{-1}\boldsymbol{f} = \boldsymbol{f} \tag{10}$$

Finally, $\boldsymbol{u}$ can be written as $\boldsymbol{u} = \mathbf{H}\boldsymbol{f}$, which provides the FRF of the unknown subsystem U:

$$\boldsymbol{u} = \left(\mathbf{Z}^{-1} - \mathbf{Z}^{-1}\mathbf{B_E}^T\left(\mathbf{B_C}\mathbf{Z}^{-1}\mathbf{B_E}^T\right)^+ \mathbf{B_C}\mathbf{Z}^{-1}\right)\boldsymbol{f} \tag{11}$$

i.e., by noting that the inverse of the block diagonal dynamic stiffness matrix can be expressed as:

$$\begin{bmatrix} \mathbf{Z^{RU}} & \mathbf{0} \\ \mathbf{0} & -\mathbf{Z^R} \end{bmatrix}^{-1} = \mathbf{Z}^{-1} = \mathbf{H} = \begin{bmatrix} \mathbf{H^{RU}} & \mathbf{0} \\ \mathbf{0} & -\mathbf{H^R} \end{bmatrix} \tag{12}$$

where $\mathbf{H^{RU}}$ and $\mathbf{H^R}$ are the FRFs of the assembled structure and of the residual substructure, it is:

$$\mathbf{H^U} = \mathbf{H} - \mathbf{H}\mathbf{B_E}^T\left(\mathbf{B_C}\mathbf{H}\mathbf{B_E}^T\right)^+ \mathbf{B_C}\mathbf{H} \tag{13}$$

With the dual assembly, the rows and the columns of $\mathbf{H^U}$ corresponding to compatibility and equilibrium DoFs appear twice. Furthermore, when using an extended or mixed interface, $\mathbf{H^U}$ contains some meaningless rows and columns: those corresponding to the internal DoFs of the residual substructure R. Obviously, only meaningful and independent entries are retained.

2.2. Interface flexibility matrix

In Eq. (13), the product of the three matrices to be inverted can be defined as interface flexibility matrix. The interface flexibility matrix can be rewritten in expanded form as:

$$\begin{bmatrix} \mathbf{B}_{\mathbf{C}}^{\mathbf{RU}} & \mathbf{B}_{\mathbf{C}}^{\mathbf{R}} \end{bmatrix} \begin{bmatrix} \mathbf{H}^{\mathbf{RU}} & \mathbf{0} \\ \mathbf{0} & -\mathbf{H}^{\mathbf{R}} \end{bmatrix} \begin{bmatrix} \mathbf{B}_{\mathbf{E}}^{\mathbf{RU}^T} \\ \mathbf{B}_{\mathbf{E}}^{\mathbf{R}^T} \end{bmatrix} = \mathbf{B}_{\mathbf{C}}^{\mathbf{RU}} \mathbf{H}^{\mathbf{RU}} \mathbf{B}_{\mathbf{E}}^{\mathbf{RU}^T} - \mathbf{B}_{\mathbf{C}}^{\mathbf{R}} \mathbf{H}^{\mathbf{R}} \mathbf{B}_{\mathbf{E}}^{\mathbf{R}^T} \tag{14}$$

It can be noticed that

$$\mathbf{B}_{\mathbf{C}}^{\mathbf{RU}} \mathbf{H}^{\mathbf{RU}} \mathbf{B}_{\mathbf{E}}^{\mathbf{RU}^T} = \hat{\mathbf{H}}^{\mathbf{RU}}$$

where $\hat{\mathbf{H}}^{\mathbf{RU}}$ is a subset of the FRF matrix of the coupled structure: premultiplication by $\mathbf{B}_{\mathbf{C}}^{\mathbf{RU}}$ extracts rows at compatibility DoFs, and postmultiplication by $\mathbf{B}_{\mathbf{E}}^{\mathbf{RU}}$ extracts columns at the equilibrium DoFs. Similarly,

$$\mathbf{B}_{\mathbf{C}}^{\mathbf{R}} \mathbf{H}^{\mathbf{R}} \mathbf{B}_{\mathbf{E}}^{\mathbf{R}^T} = \hat{\mathbf{H}}^{\mathbf{R}}$$

where $\hat{\mathbf{H}}^{\mathbf{R}}$ is the FRF of the residual structure at the same DoFs as above.

Therefore, the interface flexibility matrix becomes:

$$\mathbf{B}_{\mathbf{C}}^{\mathbf{RU}} \mathbf{H}^{\mathbf{RU}} \mathbf{B}_{\mathbf{E}}^{\mathbf{RU}^T} - \mathbf{B}_{\mathbf{C}}^{\mathbf{R}} \mathbf{H}^{\mathbf{R}} \mathbf{B}_{\mathbf{E}}^{\mathbf{R}^T} = \hat{\mathbf{H}}^{\mathbf{RU}} - \hat{\mathbf{H}}^{\mathbf{R}} \tag{15}$$

The interface flexibility matrix (15) is strictly related to singularity [7, 8].

3. Test bed

The proposed decoupling technique is tested on an aluminium tree structure (Fig. 2). The residual substructure *R* consists of a cantilever column with two staggered short arms. The unknown substructure *U* is a horizontal beam. The horizontal beam is bolted to the top of the column, involving both translational and rotational DoFs.

The geometrical dimensions are reported in Table 1. The cross section is 40 mm×8 mm for all beams, with the short side along the *z*-direction.

The experimental FRFs of the assembled system *RU* up to 2000 Hz are obtained by applying impact excitation and measuring the resulting accelerations along *z*-direction at seven locations (3, 6, 9, 10, 11, 13, 20), as shown in Fig. 3. For the residual subsystem *R* (column) the experimental FRFs are similarly measured at five locations (3, 6, 9, 10, 11), as shown in Fig. 4. A detail of the bolted junction between the beam and the column is shown in Fig. 5. Finally, to check decoupling results, FRFs are measured also at three locations (11, 13, 20) of the unknown subsystem *U* (beam), supported by an inflated rubber tube, shown in Fig. 6, giving rigid body eigenfrequencies well separated from the first flexible mode of the beam. Measurements are performed by placing the accelerometers at the underside of each (sub)structure. In order to obtain a complete FRF matrix, as required by the decoupling technique, impact excitation is sequentially provided on all DoFs at the topside of each (sub)structure.

A reciprocity check is performed on the experimental FRFs showing that reciprocity is acceptable for all FRF pairs involving coupling DoFs and internal DoFs of the residual subsystem, i.e. the DoFs that can be used to enforce compatibility and equilibrium conditions. Figures 7 and 8 show the reciprocity check on experimental FRFs of the assembled structure *RU* and of the residual subsystem *R*. No indication about possible FRFs that should be discarded because of lack of reciprocity is provided by this check.

a	*b*	*c*	*d*	*e*	*l*
540	420	60	100	240	600

Table 1: Geometrical dimensions [mm]

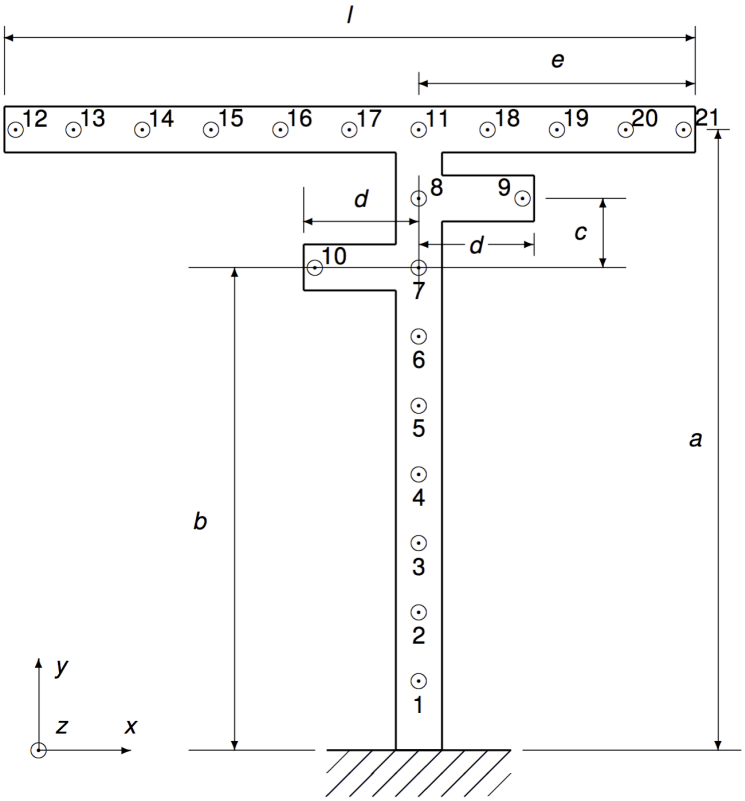

Figure 2: Sketch of the test structure.

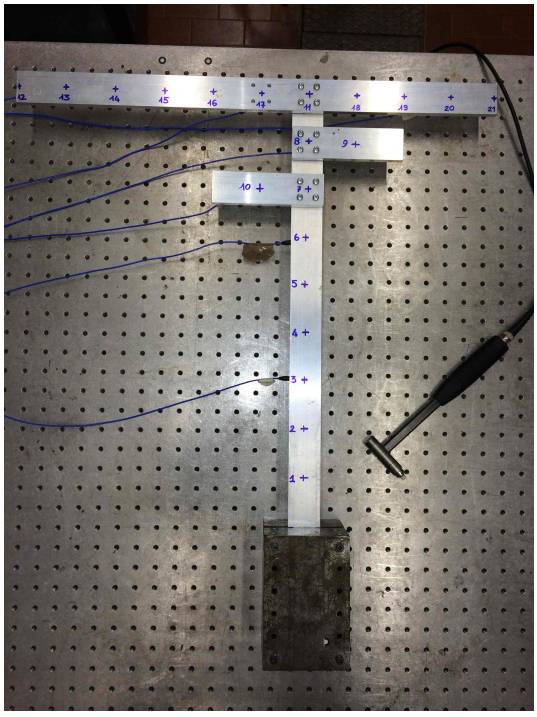
Figure 3: Assembled system.

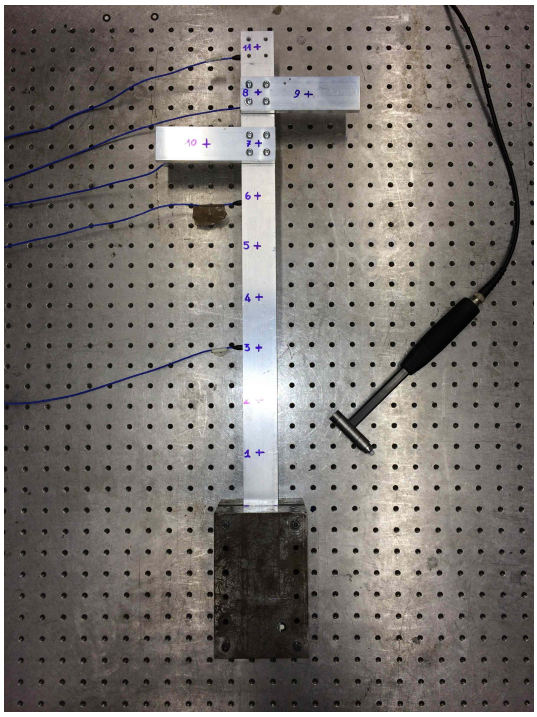

Figure 4: Residual subsystem.

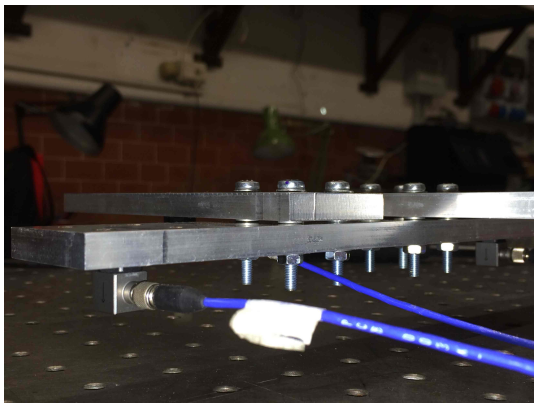

Figure 5: Detail of the bolted junction.

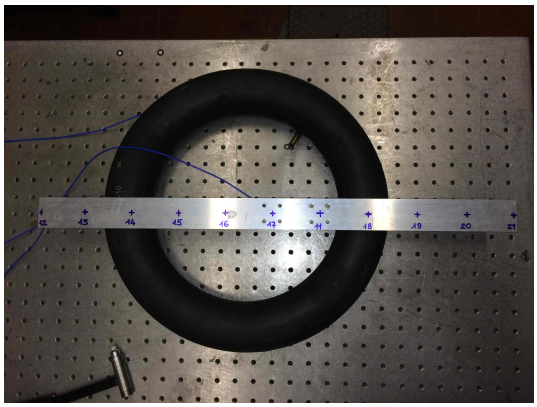

Figure 6: Unknown subsystem.

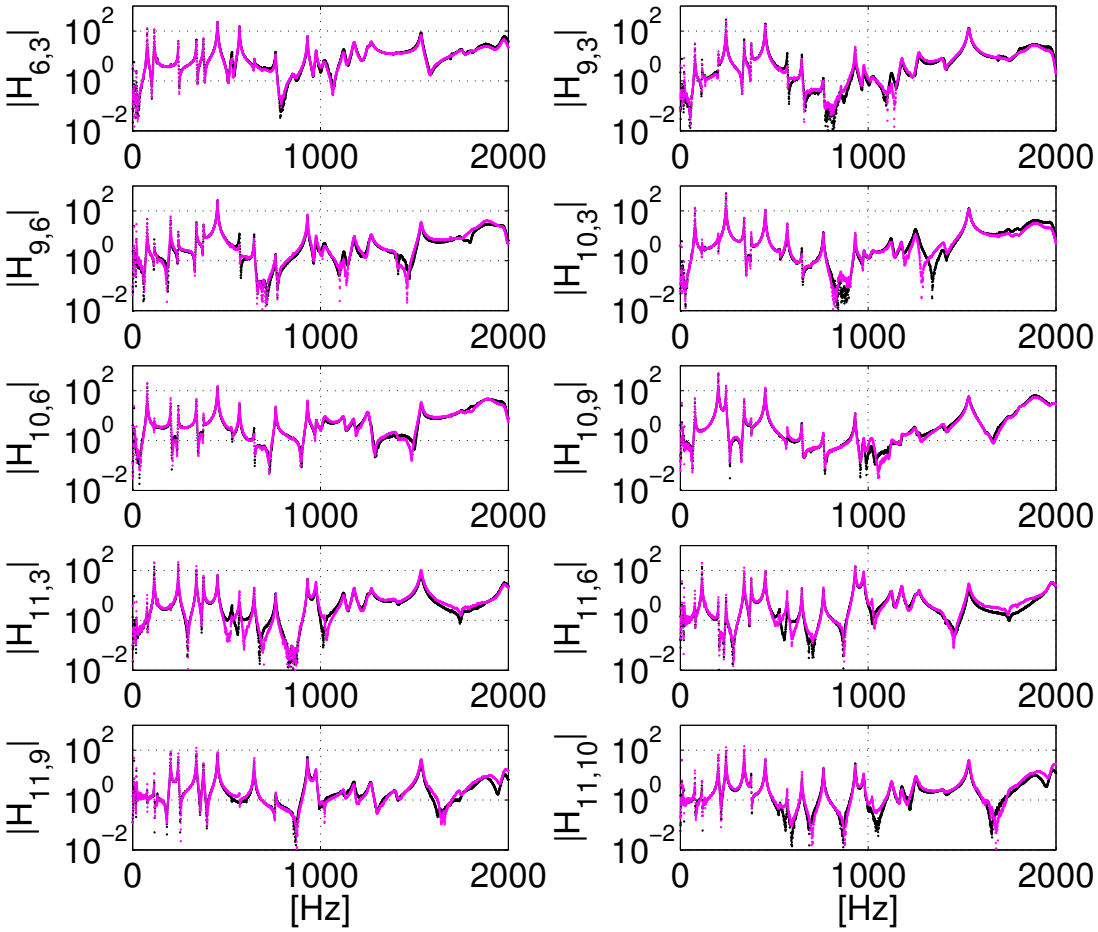

Figure 7: Reciprocity check on experimental FRFs of the assembled structure *RU* among DoFs 3, 6, 9, 10, 11.

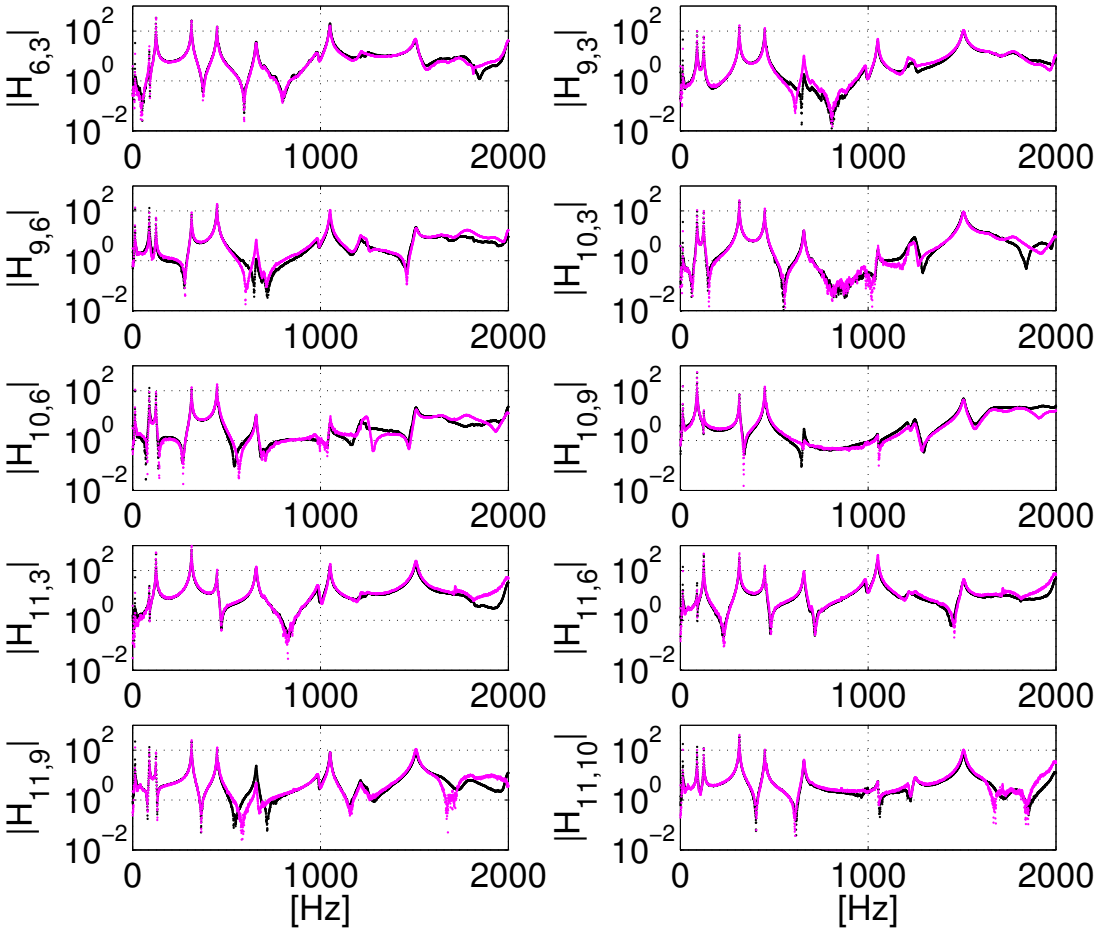

Figure 8: Reciprocity check on experimental FRFs of the residual structure *RU* among DoFs 3, 6, 9, 10, 11.

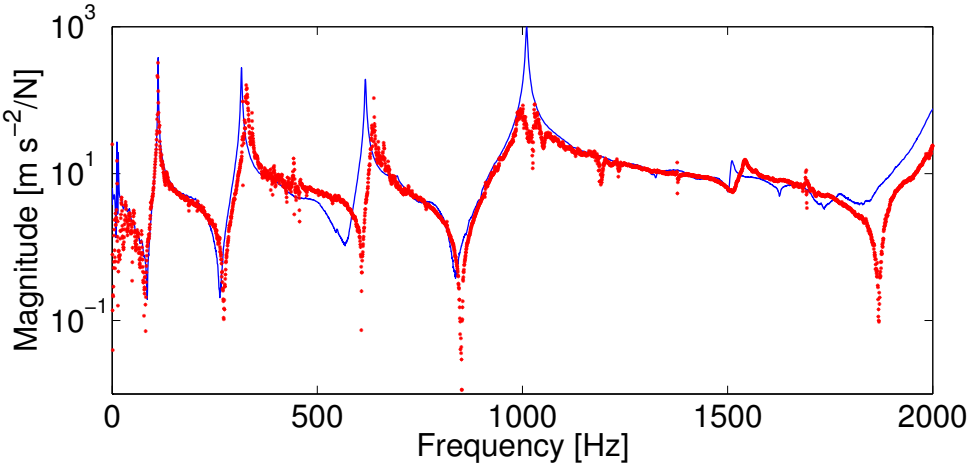

Figure 9: $H^U_{11z,11z}$: measured (—), computed using mixed interface with coupling DoF $11z$, and internal DoFs $3z$, $6z$, $9z$ (***).

4. Decoupling

The FRFs of subsystem U can be determined through the procedure described previously and summarized in Eq. (13), where compatibility and equilibrium DoFs are defined case by case. A collocated approach is adopted in which compatibility and equilibrium DoFs are the same.

Since rotational DoFs at the junction between the residual subsystem and the unknown subsystem can not be measured, neither the standard interface nor the extended interface can be used. Therefore, only mixed interfaces can be considered.

FRFs to be used in decoupling can be either the raw FRFs or can be obtained by a curve fitting procedure.

4.1. Results using raw FRFs

The number n_c of coupling DoFs is 3 so that it must be $N_E \geq n_c = 3$. To deal with overdetermined problems, a set of attempts using mixed interfaces with $N_C = N_E = 4$ is performed.

First, an interface including DoFs $3z$, $6z$, $9z$ and $11z$ is used. Therefore

$$\mathbf{B_C} = \mathbf{B_E} = \begin{array}{c} \begin{array}{cccc|cccc} u^{RU}_{3z} & u^{RU}_{6z} & u^{RU}_{9y} & u^{RU}_{11z} & u^{R}_{3z} & u^{R}_{6z} & u^{R}_{9z} & u^{R}_{11z} \end{array} \\ \left[\begin{array}{cccc|cccc} 1 & 0 & 0 & 0 & -1 & 0 & 0 & 0 \\ 0 & 1 & 0 & 0 & 0 & -1 & 0 & 0 \\ 0 & 0 & 1 & 0 & 0 & 0 & -1 & 0 \\ 0 & 0 & 0 & 1 & 0 & 0 & 0 & -1 \end{array}\right] \\ \mathbf{B^{RU}_C} \qquad\qquad \mathbf{B^{R}_C} \end{array} \tag{16}$$

The FRF of the unknown substructure U is shown in Fig. 9. It can be noticed that, although the FRF is not very scattered, the peak around 1000 Hz is not well described and some other peaks are shifted towards higher frequencies.

Another mixed interface including DoFs $3z$, $6z$, $10z$ and $11z$ is used. The signed Boolean matrices $\mathbf{B_C}$ and $\mathbf{B_E}$ are built as in the previous case. The FRF of the unknown substructure U is shown in Fig. 10. It can be noticed that around 500 Hz a spurious peak appear and another peak is considerably forward shifted. However, the peak around 1000 Hz is better described.

Subsequently, a mixed interface including DoFs $3z$, $9z$, $10z$ and $11z$ is used. The signed Boolean matrices $\mathbf{B_C}$ and $\mathbf{B_E}$ are built as in the first case. The FRF of the unknown substructure U is shown in Fig. 11. It can be noticed that around 600 Hz the peak is shifted forward and around this peak the FRF is a bit scattered. However, the peak around 1000 Hz is very well described.

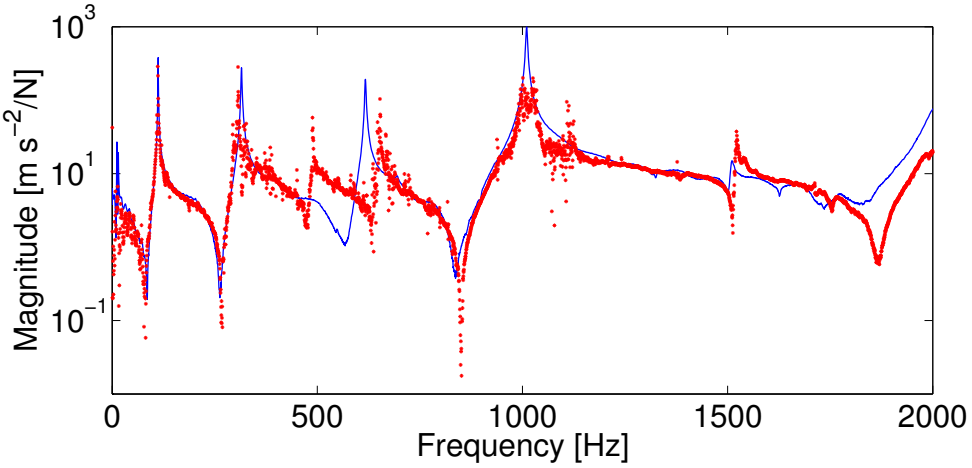

Figure 10: $H^U_{11z,11z}$: measured (—), computed using mixed interface with coupling DoF $11z$, and internal DoFs $3z$, $6z$, $10z$ (***).

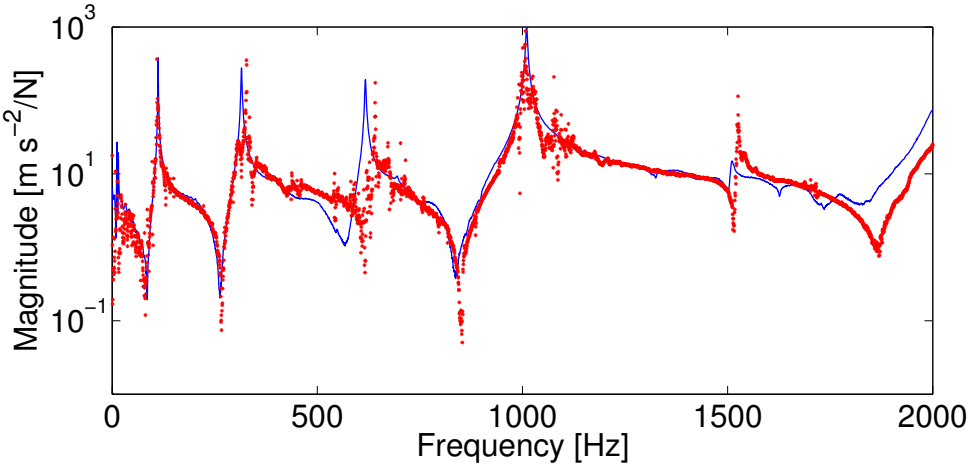

Figure 11: $H^U_{11z,11z}$: measured (—), computed using mixed interface with coupling DoF $11z$, and internal DoFs $3z$, $9z$, $10z$ (***).

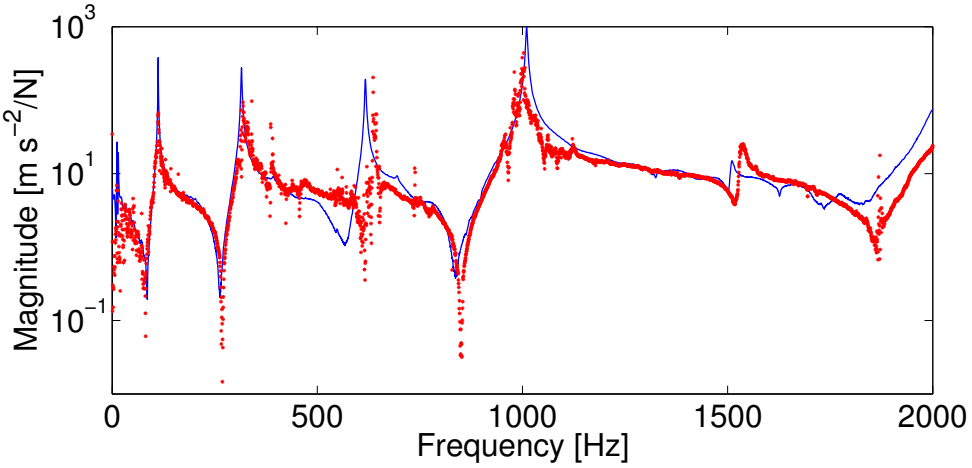

Figure 12: $H^U_{11z,11z}$: measured (—), computed using mixed interface with coupling DoF $11z$, and internal DoFs $6z$, $9z$, $10z$ (⁎⁎⁎).

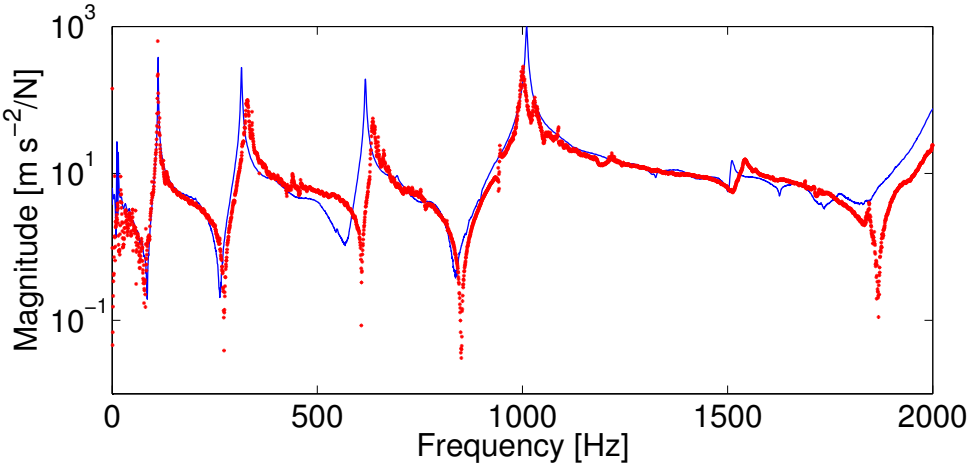

Figure 13: $H^U_{11z,11z}$: measured (—), computed using mixed interface with coupling DoF $11z$, and internal DoFs $3z$, $9z$ (⁎⁎⁎).

Finally, a mixed interface including DoFs $6z$, $9z$, $10z$ and $11z$ is used. The signed Boolean matrices $\mathbf{B_C}$ and $\mathbf{B_E}$ are built similarly to the first case. The FRF of the unknown substructure U is shown in Fig. 12. At a first glance, the result looks very similar to the previous one (interface DoFs $3z$, $9z$, $10z$ and $11z$), but it is definitely worse because of several spikes and because the FRF around 1000 Hz is described less accurately than in the previous case.

A new set of attempts is performed using mixed interfaces including only 3 DoFs that give rise to determined problems. Based on the previous results, a mixed interface that includes DoFs $3z$, $9z$ and $11z$ is used. Such DoFs represent the set intersection between DoFs $3z$, $6z$, $9z$, $11z$ and $3z$, $9z$, $10z$, $11z$ that provide the best results using 4 interface DoFs. The signed Boolean matrices $\mathbf{B_C}$ and $\mathbf{B_E}$ are built similarly to the first case. The FRF of the unknown substructure U is shown in Fig. 13. It can be noticed that the result is quite clean with no significant drawbacks.

To cross-check this result, a mixed interface that includes DoFs $6z$, $10z$ and $11z$ is used. Such DoFs represent the set intersection between DoFs $3z$, $6z$, $10z$, $11z$ and $6z$, $9z$, $10z$, $11z$ that provide the worst results using 4 interface DoFs. The FRF of the unknown substructure U is shown in Fig. 14. It can be noticed that the result is quite bad with significant scatter around the natural frequencies and several spurious peaks.

A further check is performed using a mixed interface that includes DoFs $9z$, $10z$ and $11z$. DoFs $9z$, $10z$ are both able to provide information about the rotational DoF θ_y (torsion of the column) but may miss the information about the rotational DoF θ_x (bending of the column). The FRF of the unknown substructure U is shown in Fig. 15. It can be

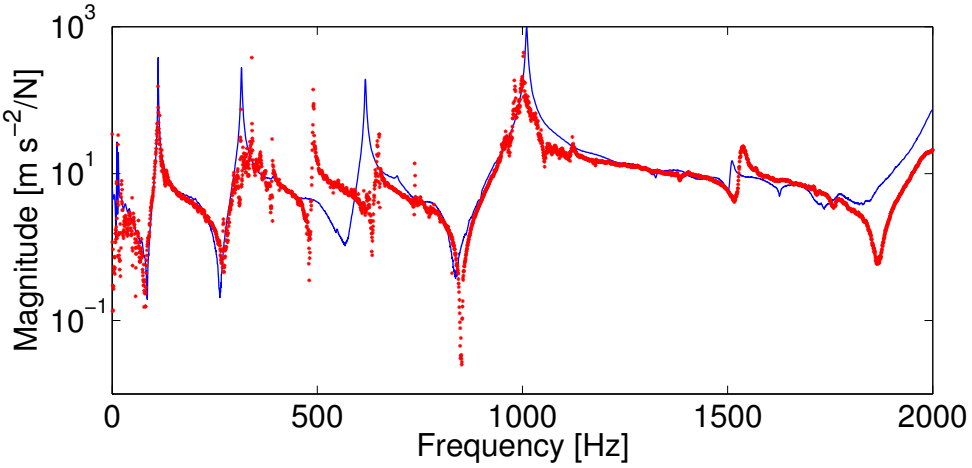

Figure 14: $H^U_{11z,11z}$: measured (—), computed using mixed interface with coupling DoF $11z$, and internal DoFs $6z$, $10z$ (***).

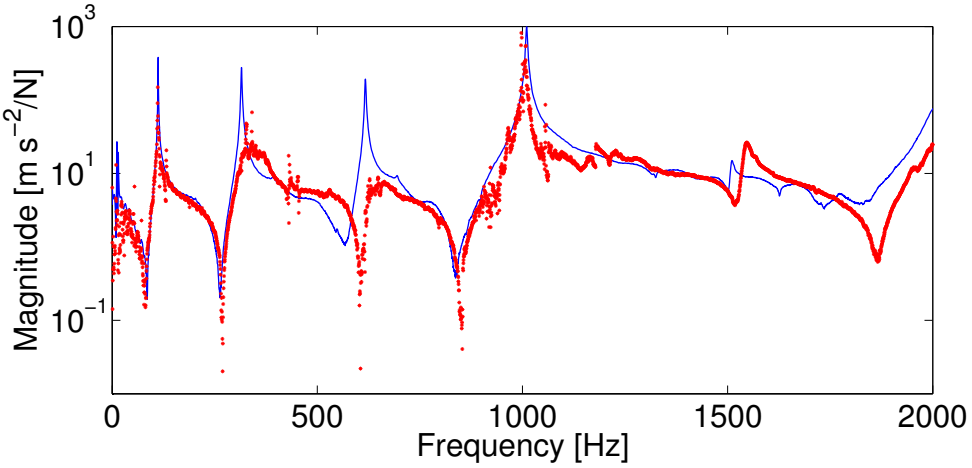

Figure 15: $H^U_{11z,11z}$: measured (—), computed using mixed interface with coupling DoF $11z$, and internal DoFs $9z$, $10z$ (***).

noticed that the result is very bad because the two modes around 315 Hz and 615 Hz are not clearly visible.

4.2. Results using fitted FRFs

It is usually believed that the use of curve fitted FRFs, due to the smoothing effect on experimental noise, is able to provide better results. Therefore, a curve fitting is performed using a poly-reference least square complex frequency domain technique [14] that allows to deal with a consistent FRF matrix. The modal identification is performed from 40 up to 1100 Hz, which is the most interesting range for decoupling. The curve fitting results for the FRFs at DoFs 3, 9 and 11 of the assembled structure RU show a good quality of the fitting (see Fig. 16). Similar results are obtained for the residual structure R at the same DoFs (see Fig. 17).

First, the mixed interface including DoFs $3z$, $6z$, $9z$ and $11z$ is used. It provides one of the best results with raw FRFs and four interface DoFs. The FRF of the unknown substructure U is shown in Fig. 18. It can be noticed that, although the first peak around 110 Hz is well described, other peaks are shifted towards higher frequencies and are not very sharp.

Subsequently, the mixed interface including DoFs $3z$, $9z$ and $11z$ is used, that provides the best result with raw FRFs. The FRF of the unknown substructure U is shown in Fig. 19. It can be noticed that the result is very similar to

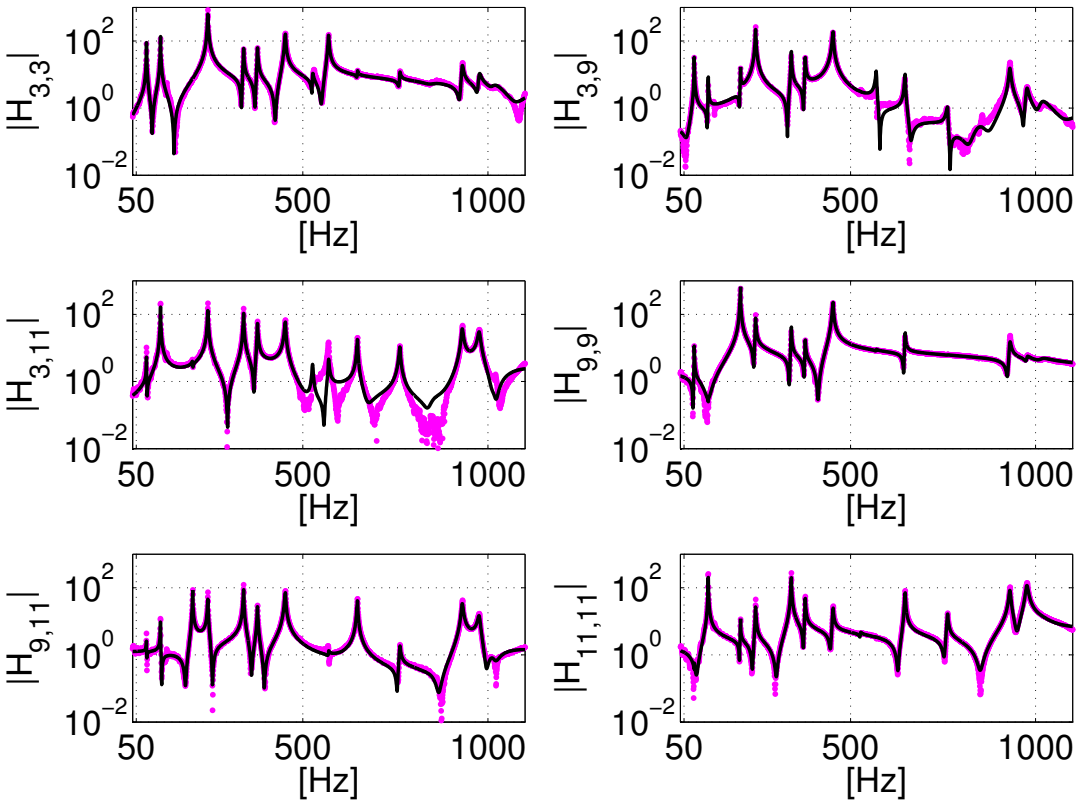

Figure 16: Comparison between experimental (▪▪▪) and fitted FRFs (—) of the assembled structure *RU* at DoFs 3, 9, 11.

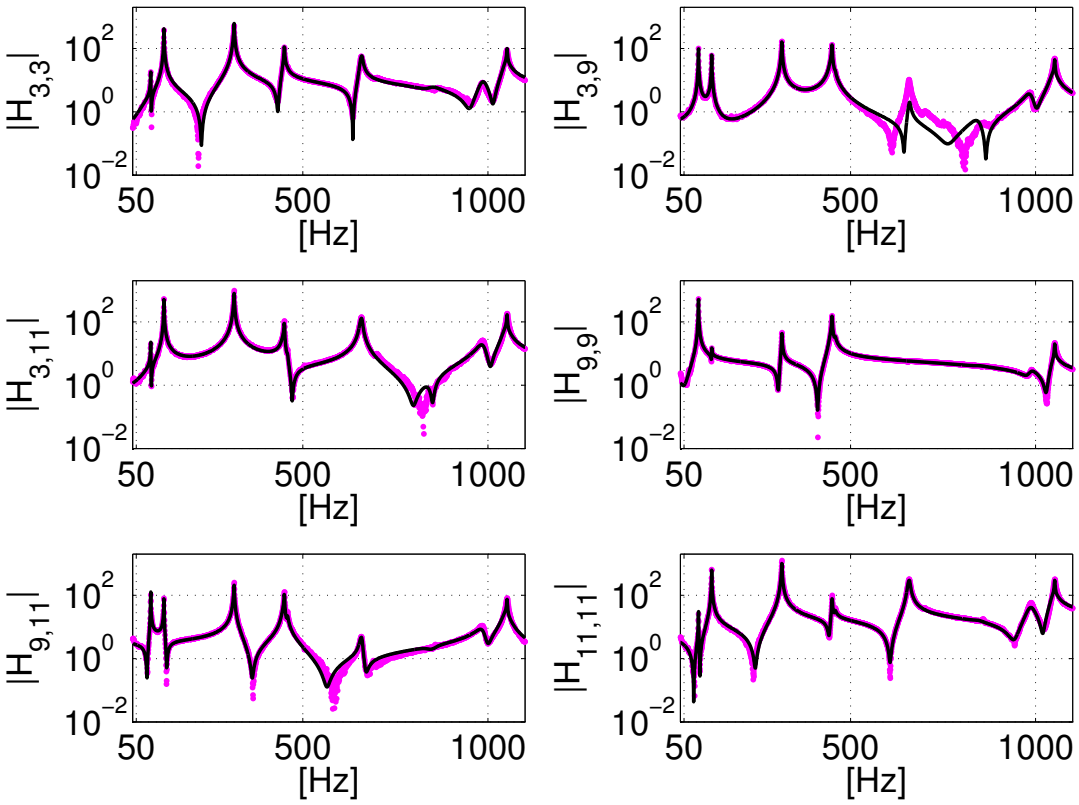

Figure 17: Comparison between experimental (•••) and fitted FRFs (—) of the residual structure R at DoFs 3, 9, 11.

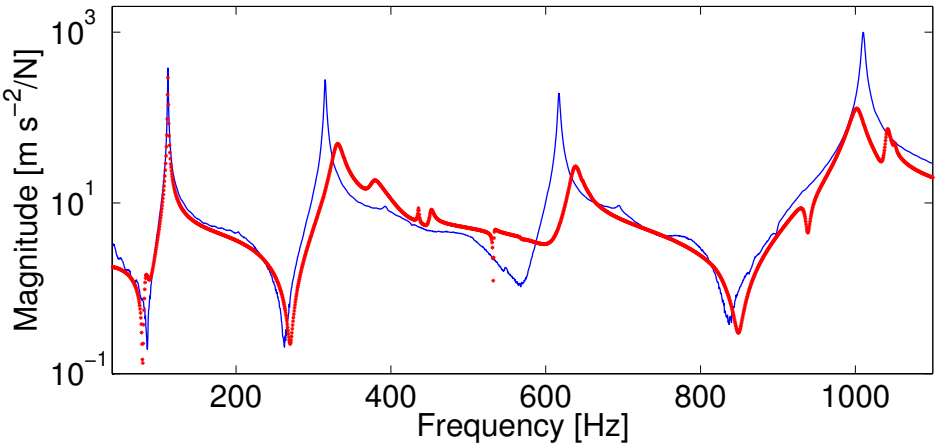

Figure 18: $H^{U}_{11z,11z}$: measured (—), computed using mixed interface with coupling DoF $11z$, and internal DoFs $3z$, $6z$, $9z$ (•••).

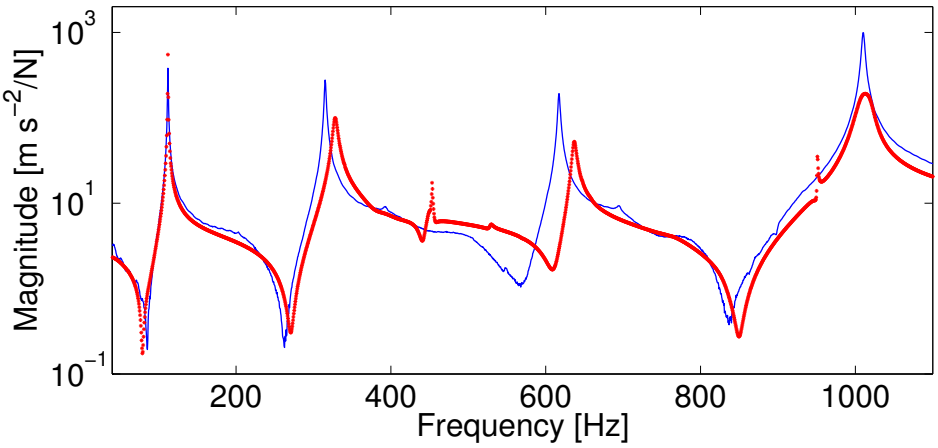

Figure 19: $H^U_{11z,11z}$: measured (—), computed using mixed interface with coupling DoF $11z$, and internal DoFs $3z$, $9z$ (***).

that obtained with raw FRFs apart from the spurious small peak around 450 Hz which is slightly more evident in this case.

However, with other combinations of interface DoFs, the results obtained using curve fitted FRFs are definitely worse than those obtained using raw FRFs and are not shown in the paper.

5. Concluding remarks

In this paper, it is tried to establish if rotational DoFs, possibly included among the connecting DoFs, are essential in substructure decoupling, not only from a theoretical side but also when dealing with experimental data.

Differently from the coupling problem, where rotational DoFs can not be neglected, in the decoupling case this is possible because the actions exchanged through the connecting DoFs, and specifically through rotational DoFs, are already embedded in each FRF of the assembled system. In the decoupling case, a mixed or a pseudo interface can in fact be considered that allow to substitute undesired coupling DoFs with internal DoFs of the residual subsystem.

The procedure is verified on an experimental test bed. The test bed is a tree structure made by a cantilever column with two staggered short arms coupled to a horizontal beam. This involves both flexural and torsional DoFs, on which rotational FRFs are quite difficult to measure. Using a mixed interface, such FRFs are neglected and substituted by FRFs involving internal translational DoFs.

FRFs to be used in decoupling can be either the raw FRFs or can be obtained by a curve fitting procedure. It is typically believed that the use of curve fitted FRFs, due to the smoothing effect on experimental noise, is able to provide better results. However, in this application this is not true: only in the two cases shown in the paper, results are comparable to (but slightly worse than) those obtained using raw FRFs at the same interface DoFs. By looking at the results obtained using raw FRFs, it can be noticed that increasing the number of interface DoFs to deal with an overdetermined problem does not necessarily improve the estimate of the unknown FRFs. Conversely, decreasing the number of interface DoFs may lead to better results but increases the variability of the estimates.

Acknowledgements

This research is supported by grants from University of Rome La Sapienza and University of L'Aquila.

References

[1] D. de Klerk, D. J. Rixen, S. Voormeeren, General framework for dynamic substructuring: History, review, and classification of techniques, AIAA Journal 46 (2008) 1169–1181.

[2] A. Sestieri, P. Salvini, W. D'Ambrogio, Reducing scatter from derived rotational data to determine the frequency response function of connected structures, Mechanical Systems and Signal Processing 5 (1991) 25–44.
[3] A. Stanbridge, D. Ewins, Measurement of translational and angular vibration using a scanning laser doppler vibrometer, Shock and Vibration 3 (1996) 141–152.
[4] M. Bello, A. Sestieri, W. D'Ambrogio, F. La Gala, Development of a rotational transducer based on bimorph PZT's, Mechanical Systems and Signal Processing 17 (2003) 1069–1081.
[5] W. D'Ambrogio, A. Fregolent, Promises and pitfalls of decoupling procedures, in: Proceedings of 26th IMAC, Orlando (U.S.A.), 2008.
[6] P. Sjövall, T. Abrahamsson, Substructure system identification from coupled system test data, Mechanical Systems and Signal Processing 22 (2008) 15–33.
[7] W. D'Ambrogio, A. Fregolent, The role of interface DoFs in decoupling of substructures based on the dual domain decomposition, Mechanical Systems and Signal Processing 24 (2010) 2035–2048.
[8] W. D'Ambrogio, A. Fregolent, Direct decoupling of substructures using primal and dual formulation, in: Conference Proceedings of the Society of Experimental Mechanics Series, Volume 4, Linking Models and Experiments, volume 2, Springer, Jacksonville, Florida USA, 2011, pp. 47–76. doi:10.1007/978-1-4419-9305-2_5.
[9] W. D'Ambrogio, A. Fregolent, Inverse dynamic substructuring using direct hybrid assembly in the frequency domain, Mechanical Systems and Signal Processing 45 (2014) 360–377.
[10] W. D'Ambrogio, A. Fregolent, Identification of interface forces for inverse dynamic substructuring applications, in: P. Sas, D. Moens, H. Denayer (Eds.), Proceedings of ISMA 2014 - International Conference on Noise and Vibration Engineering, Leuven (Belgium), 2014, pp. 3855–3868.
[11] S. N. Voormeeren, D. J. Rixen, A family of substructure decoupling techniques based on a dual assembly approach, Mechanical Systems and Signal Processing 27 (2012) 379–396.
[12] W. D'Ambrogio, A. Fregolent, Are rotational DoFs essential in substructure decoupling?, in: M. Allen, R. Mayes, D. Rixen (Eds.), Dynamics of Coupled Structures, Volume 1, Conference Proceedings of the Society for Experimental Mechanics Series, Springer International Publishing, 2014, pp. 27–36. URL: http://dx.doi.org/10.1007/978-3-319-04501-6_3. doi:10.1007/978-3-319-04501-6_3.
[13] W. D'Ambrogio, A. Fregolent, Ignoring rotational dofs in decoupling structures connected through flexotorsional joints, in: M. Allen, R. L. Mayes, D. J. Rixen (Eds.), Dynamics of Coupled Structures, Volume 4, Conference Proceedings of the Society for Experimental Mechanics Series, Springer International Publishing, 2015, pp. 57–69. URL: http://dx.doi.org/10.1007/978-3-319-15209-7_6. doi:10.1007/978-3-319-15209-7_6.
[14] A. Culla, W. D'Ambrogio, A. Fregolent, Getting a symmetric residue matrix from the poly-reference least square complex frequency domain technique, in: P. Sas (Ed.), Proceedings of ISMA 2012 - International Conference on Noise and Vibration Engineering, Leuven (Belgium), 2012, pp. 2755–2764.